Energy Proceedings
Vol 30, 2023
ISSN 2004-2965

Planning Building Integrated Photovoltaics (BIPV) Adapting to Extreme Wind Weather

Zhengguang Liu[1,2], Ying Du[3], Zhiling Guo[1*], Chenchen Song [4], Qi Chen[5], Wene Wang[2], Haoran Zhang[1]

1 Center for Spatial Information Science, University of Tokyo, Kashiwa 277-8568, Japan (Corresponding Author)

2 Department of Power and Electrical Engineering, Northwest A&F University, Yangling, 712100, China

3 State Energy Smart Grid (Shanghai) R&D Center, Shanghai Jiao Tong University, Shanghai, 200240, China

4 Research Center for Energy Transition and Social Development, Tsinghua University, Beijing 100084, China

5 School of Geography and Information Engineering, China University of Geosciences (Wuhan), China

ABSTRACT

The dual-carbon target has made solar photovoltaic panels widely used. But the normal operation of photovoltaic panels under extreme weather conditions is still an important issue to be solved. For large-area photovoltaic arrays, the effect of photovoltaic panels under extreme wind weather, such as typhoon, is becoming more obvious. To solve the above dilemma, this paper established the numerical simulation model of photovoltaic panels under turbulence field, and studied the displacement of the solar panels when the wind speed is over 25m/s. The results have shown that when the flow rate is 25m/s, the maximum relative pressure of the solar panel is about 70Pa, which appears on the upper right and left of the solar panel. The maximum displacement caused by the wind also appears on the same point of the solar panel, which even reached 1mm in solid surface. After this the economic analysis has also been done for PV operation and maintenance. The machine replacement rate data dropped from 5.6% to 1.7% after added the reinforced facilities. The LCOE for PV also reduced. These results can provide an important reference for the planning of solar panels and the effective operation under extreme weather conditions like typhoon in the future.

Keywords: Renewable energy resources, Advanced energy technologies, Solar panel; Building Integrated Photovoltaics; Fluid-structure interaction, Climate change

NONMENCLATURE

Abbreviations	
PV	Photovoltaic
Symbols	
y_g	Atmospheric boundary layer height
U_{gis}	Geostrophic wind velocity
y	Distance
α	Exponent dependent on the terrain
It	investment expenditures in year t;
r	discount rate
E_t	Electrical energy generated in year t
F_t	Fuel expenditures in the year t
M_t	Operations and maintenance expenditures in the year t
σ	Equipment replacement rate
μ	Component failure rate

1. INTRODUCTION

Solar energy utilization has become the research hotspot in academia and engineering with the proposal of dual-carbon target in China [1] [2]. However, in coastal cities like Rizhao, Xiamen, and other cities, a major reason for the damage in photovoltaic solar panels is that these coastal areas are often affected by extreme wind weather such as typhoons and hurricanes. These extreme wind weather made solar panels are unable to maintain normal conditions [3]. PV panels in landscape format placed on commercial buildings or flat ground are typically arranged in arrays supported by elevated steel or aluminum frames at an angle between twenty and forty degrees [4]. This tilt allows photovoltaic panels to receive more radiation, but also makes photovoltaic panels more damaged in extreme wind conditions [5] [6]. Ladas et al. [7] had made a tunnel study of wind effects on the performance of solar collectors on rectangular flat roofs, the results shown solar collectors at different locations could vary by more than 20% effected by wind, but the impact of the photovoltaic panel is not taken into consideration. Pratt et al. [8] made the velocity

measurements around low-profile, tilted, solar arrays mounted on large flat-roofs, but the reason of the change of wind speed has not be analyzed. Geurts et al. [9] analyzed the wind loads on stand-off photovoltaic systems on pitched roofs, but the results of the PV modules damage are not take into considered. The peak wind loads on tilted flat solar panels mounted on large, flat roofs are also analyzed by Banks' paper[10], but the maximum pressure of single plane are not pointed out.

To better planning solar panel adapting to extreme wind weather, this paper established the solar panels in the periodic wind field. Experiments are also carried to solve the wind flow around the solar panels. the pressure on the solar panels due to strong wind. The displacement got by this paper can be used to provide a reference for the structural design of the solar panel and material selection.

2. METHOD

2.1 Model definition

In order to effectively simulate the above situation and reduce computing time and computing power, periodic flow can be used for simplification. Periodic flow refers to the introduction of fluid into a geometric body. As shown in Figure 1, in COMSOL 5.6, the periodic flow boundary conditions are selected to simulate the arrangement of large photovoltaic generator sets. At the same time, we set the free flow velocity above the solar panels to 25 M/s (90 Km/h). The Reynolds number based on the height of the panel structure and the free flow velocity is about 6.6 ×106.

A wind velocity of 25 m/s at the height of 10 m was selected to simulate the extreme wind weather. Under this wind speed, flowers and plants can be uprooted, to simulate this inlet condition, a power-law equation (1) is used.

$$\frac{u(y)}{U_g} = \left(\frac{y}{y_g}\right)^{\alpha} \tag{1}$$

Where, y_g (300m) is the atmospheric boundary layer height of the terrain; U_{gis} the geostrophic wind velocity; α (0.16) is an exponent dependent on the terrain; y is the distance from the ground. In the current study an open terrain was considered.

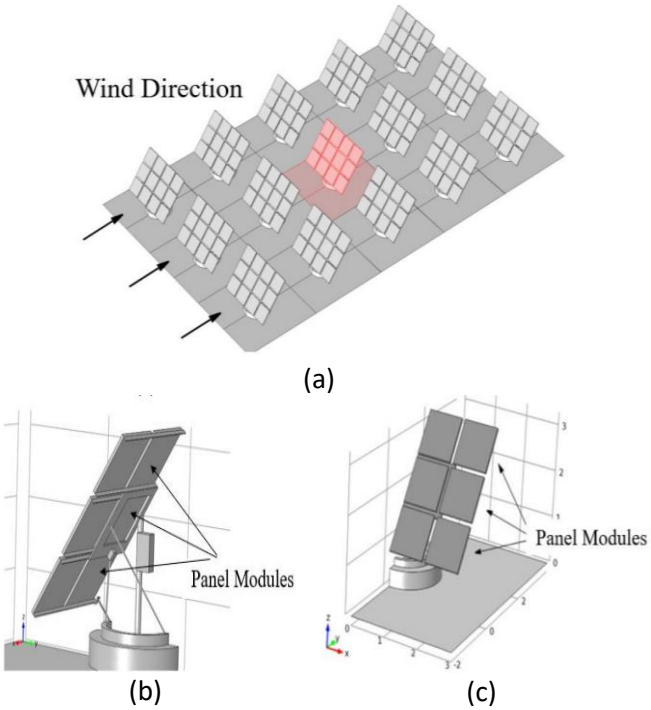

Figure 1. The modeled solar panel in buildings. (a) located in a regular array of identical panels (in red). (b) Rear view (c) Front view

2.2 Meshing and convergence settings

In this model, the mapping grid on the solar panel and refine the flow field. Periodic flow conditions are used to specify the pressure difference in the direction of flow to ensure that the average velocity at the top is 25m/s. Use the ordinary differential calculator to obtain the pressure drop required for the required free flow velocity. The top boundary is modeled by boundary stress conditions. By making the isotropic diffusion inversely proportional to the number of CFLs (CFL, convergence condition judgment number) used for pseudo time stepping, the convergence of the first iteration of the nonlinear solver is guaranteed.

The CFL starts from a lower value and increases as the resolution process progresses, until it over 1000. In the direction of flow, a periodic flow condition with a prescribed pressure difference is applied. In the lateral condition, since the solar panel structure is assumed to be symmetric, only the symmetric boundary conditions need to be applied in the lateral direction. In addition to solving the momentum and continuity equations for velocity and pressure, the Detached Eddy Simulation (DES) method should be used to calculate the turbulence from the following transport equations:

$$\begin{cases} \frac{\partial}{\partial t}(\rho k)+\frac{\partial}{\partial x_i}(\rho k u_i)=\frac{\partial}{\partial x_j}\left(\Gamma_k \frac{\partial k}{\partial x_j}\right)+G_k-Y_k+S_k \\ \frac{\partial}{\partial t}(\rho \omega)+\frac{\partial}{\partial x_i}(\rho \omega u_i)=\frac{\partial}{\partial x_j}\left(\Gamma_\omega \frac{\partial \omega}{\partial x_j}\right)+G_\omega-Y_\omega+S_\omega \end{cases} \quad (2)$$

In equation (2), u_i is the velocity component in the x_i(i=1, 2, 3) direction, k is the turbulence kinetic energy, ω is the specific dissipation rate, G_k represents the generation of k, G_ω represents the generation of ω,Γ_ω,and Γ_k represent the effective diffusivity of k and ω,Y_k and Y_ω are the dissipation of k and ω. S_k and S_ω are defined based on DES method. The top boundary condition uses the momentum equation to apply the normal stress condition to specify the flow of the top boundary layer type. At the same time, it can be assumed that the viscous stress at the top position is small, and the stress is determined according to the linear decrease of the pressure from the inlet to the outlet. The *Computational box used in the fluid-flow simulation has been shown in figure 2.* the dissipation term in Eq.(2)is written as:

$$Y_k = \rho\beta^* k\omega F_{DES} \quad (3)$$

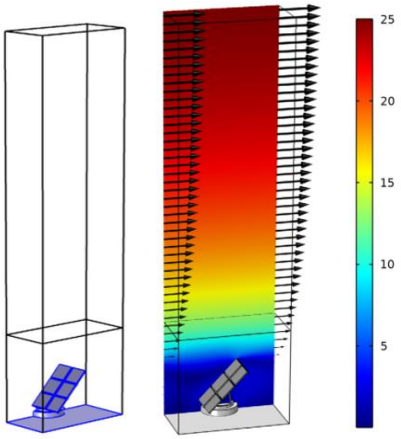

Figure 2. Computational box used in the fluid-flow simulation.

Where $\beta^*$is a constant of the SST model. The turbulent kinetic energy and dissipation rate applied at the inlet is based on the equations:

$$\begin{cases} k(y)=\frac{u_{ABL}^{*2}}{\sqrt{C_\mu}} \\ \varepsilon(y)=\frac{u_{ABL}^{*3}}{ky} \end{cases} \quad (4)$$

Where u^*_{ABL} is the atmospheric boundary layer friction velocity, k is the von Karman constant (0.40-0.42). C_μ is a model constant. In the case of the k-ω SST turbulence model, these profiles are combined to provide the specific dissipation rate ω.

2.3 Solid material selection

Single solar panel is modeled as a material with a stiffness of 3.5 GPa (5% of the stiffness of solid aluminum) and a Poisson's ratio of 0.33. Von Mises is used for ductile materials (aluminum and structural steel), and Rankine is used for glass. The stiffness of structural steel is 270MPa, glass is 250MPa, and glass is 45MPa. For the safety of, it is assumed that the compressive strength of the glass is equal to its tensile strength. The computational box of solar panel has been shown in figure2.

3. ECONOMIC ANALYSIS

3.1 Operation and maintenance cost

Strong wind means greater design and maintenance costs. For PV design, adding reinforcement equipment for strong wind can effectively reduce equipment damage and improve equipment utilization. The operation and maintenance of PV equipment can be mainly divided as routine inspection, repair of damaged parts, and replacement of damaged equipment. Figure 3 given the reinforcement structures that usually used, which would bring the increasing of installation cost and decreasing in PV loss rate.

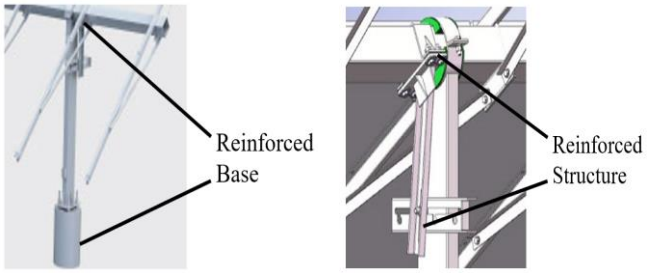

Figure 3. Photovoltaic reinforcement equipment for strong wind. (a) base (b) bracket

3.2 Levelized cost of electricity for extreme weather

Levelized Cost of Electricity (LCOE) is often used as a measure of the average net current cost of PV to generate electricity over its lifetime. The LCOE is widely used in investment planning and economic analysis, which can be express as following:

$$\mathrm{LCOE}=\frac{\sum_{t=1}^{n}\frac{I_t+M_t+F_t}{(1+r)^t}}{\sum_{t=1}^{n}\frac{E_t}{(1+r)^t}} \quad (5)$$

In equation 5, I_t is the investment expenditures in the year t; M_t is the operations and maintenance expenditures in the year t; F_t is the fuel expenditures in the year t; E_t is the electrical energy generated in the year t; r is the discount rate; n is the expected lifetime of system or power station. But when PV is set in the extreme weather, this equation should also change, the novel model for LCOE used for PV under extreme weather can be expressed as following:

$$\begin{cases} M_t' = \sum_{i=1}^{n} (M_t + X_t) \\ X_t = X(\sigma + \mu) \end{cases} \quad (6)$$

In equation 6, M_t is the operations and maintenance expenditures in the year t; σ is the equipment replacement rate under extreme weather; μ is the Component failure rate under extreme weather; X is the number of PV; X_t is the operations and maintenance expenditures for PV damage.

4. RESULTS AND DISCUSSION

4.1 Pressure Distribution

Figure 4 showed the surface fluid pressure contour and in-plane velocity components 6 cm behind the solar panel under strong wind conditions. From the figure, we can see that the surrounding airflow puts pressure on the solar panel structure. The maximum relative pressure is 70Pa, which appears in the upper right corner of the panel. This is consistent with our conventional cognition.

In order to distinguish this situation more accurately, we can find the reason for the maximum pressure in the upper right corner by drawing the in-plane velocity component on a plane perpendicular to the flow direction. After the strong wind passes through the solar panel, a large flow vortex will be generated, the center of which is aligned with the outer side of the panel. In the upper right corner, the high pressure is related to the high deflection of the air flow and the formation of the flow vortex.

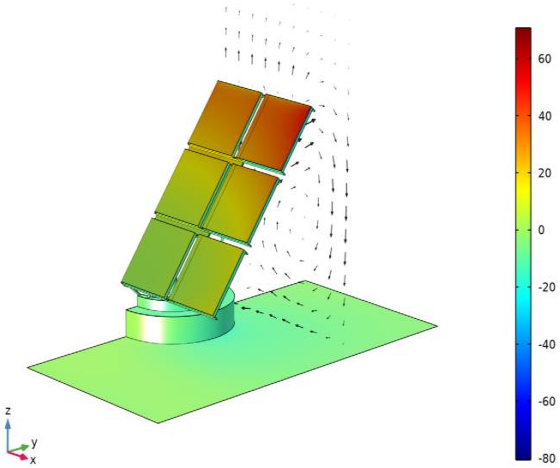

Figure 4. Surface fluid pressure contours present and in-plane velocity components 6 cm behind the panel

4.2 Velocity streamlines

The airflow around the solar panel is shown in Figure 5, showing the flow lines at the inlet. It is worth noting that some streamlines near the center of the solar panels enter this area and then turn away, which indicates that there is a circulation zone between the panels in the array. The streamlines are colored with local turbulent kinetic energy to normalize the kinetic energy of the free flow. As we predicted, the kinetic energy of the circulation area before the plate and the flow tail after the plate is lower because they are part of the same flow structure. Turbulence energy increases with distance from the ground, especially when the air flow passes over the top of the panel. The high kinetic energy at this location is related to the gradient of the average flow velocity, as set in Figure 2.

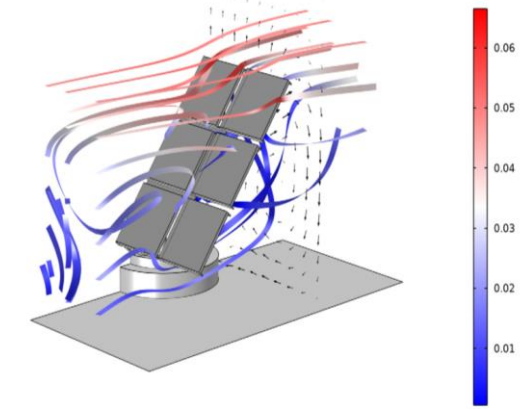

(a)

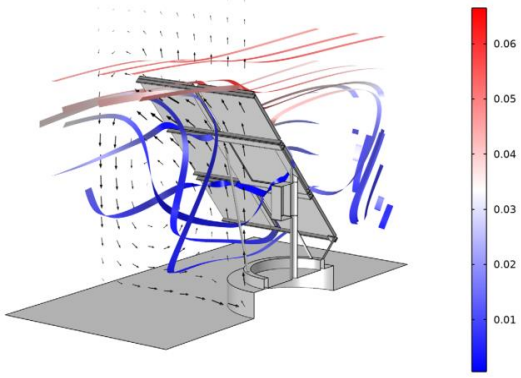

(b)

Figure 5. Velocity streamlines and in-plane velocity components. (a) front of the plane (b) back of the plane

4.3 Fluid-structure coupling distribution

Figure 6 shows the final displacement of the detailed solar panel structure in the extreme wind speed field and

the velocity streamline around the entire panel. Corresponding to the pressure diagram in Figure 4, the maximum displacement appears in the upper right corner of the diagram. However, the maximum displacement is very small, about 1MM. But for solids, this is enough to cause great damage. But at the same time, the solar panels have not been damaged, indicating that the surrounding solar panels have effectively shielded the oncoming flow of the solar panels.

For solar panels located in a large array, at the current free flow speed, the fluid load on the structure is not sufficient to determine the design of the structure, and the minimum safety factor obtained by calculation is far greater than 1. Therefore, it may be more noteworthy to design a more reasonable arrangement and distribution of solar panels. The Structural displacement of the solar panel due to the fluid-flow load, and velocity streamlines colored by the velocity magnitude has been shown in figure 6 and table 1.

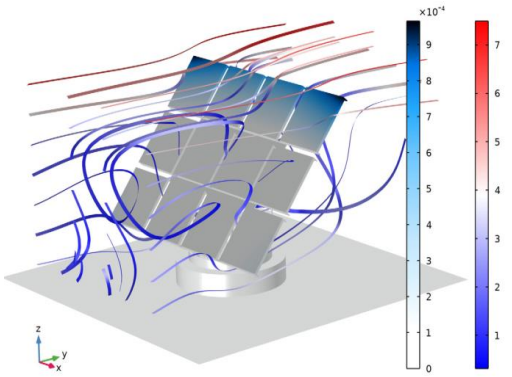

Figure 6. Structural displacement of the solar panel due to the fluid-flow load, and velocity streamlines colored by the velocity magnitude

The results of solar plane in extreme windy weather have been shown in table 1, which can be used to planning the solar panel adapting to extreme wind weather.

Table 1 Solar plane results in extreme windy weather

Performance of solar plane		
Maximum wind speed	**Maximum displacement**	**Minimum safety factor**
25.7m/s	1mm	1.23

4.4 Failure rate for PV under extreme weather

After installed the reinforced facilities, the failure and damage rate of photovoltaic equipment in extreme weather has dropped significantly. This paper selects the failure rate data from Rizhao in Shandong Province for comparative analysis. The PV equipment failure rate changes with reinforced facilities has been shown in figure 7.

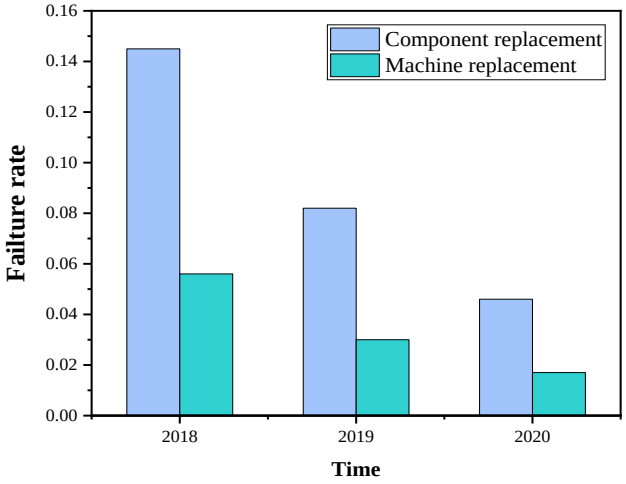

Figure 7. The PV equipment failure rate changes with reinforced facilities installation in Rizhao (2018:0%; 2019 50%; 2020 100%)

After installed the reinforced facilities, the component damage rate of PV has dropped significantly from over 14% to 4.6%. The Machine replacement rate data dropped from 5.6% to 1.7%. The effective reduction of PV equipment failure rate proves the effectiveness of the installed maintenance equipment.

4.5 LCOE for PV panels

The relevant results of LCOE have been shown in Figure 8. In coastal cities such as Rizhao, due to the influence of extreme wind weather, the actual LCOE value is usually higher than the market. The LCOE in Rizhao is 0.47 ￥/kWh, but after the installation of reinforced facilities, this value is reduced to 0.44￥/kWh. Although this value is still higher than the market price of 0.44 ￥/kWh, the effectiveness and robustness of the PV with reinforced facilities have been verified.

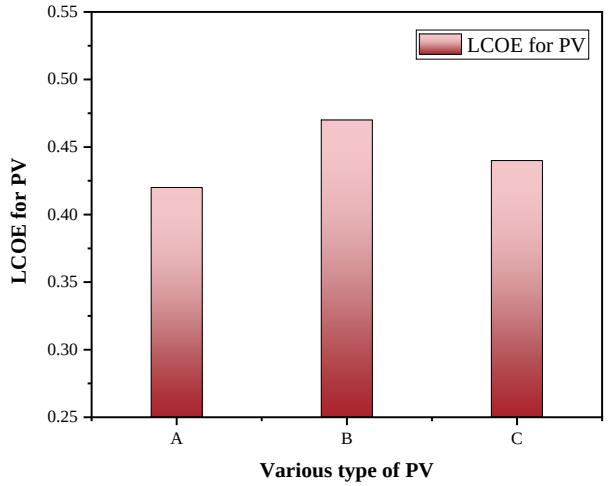

Figure 8. The LCOE of PV with different types installation in Rizhao (A: LCOE in China; B: LCOE in Rizhao; 2020 LCOE for PV with reinforced facilities in Rizhao)

5. CONCLUSION

In this paper, a numerical simulation analysis model suitable for solar farms under extreme wind weather was established. Through the setting of boundary conditions, it can be used to simulated the actual performance of solar plane under extreme wind weather conditions, especially when the wind speed is greater than 25m/s, the results can be summed as followed.

(1) The solar panel received the greatest force lies on the top left and right, and the maximum relative pressure on this point is about 70PA. The specific pressure is related to the vortex formed by the wind flowing through the solar panel.

(2) The displacement caused by wind speed can reach 1mm, which will bring great damage to solid planes. Further consideration should be given to the replacement and filling of materials at the corners.

(3) After the installation of reinforced facilities, the LCOE of PV can reduce to 0.44￥/kWh. the reinforced facilities can effectively reduce the failure rate of PV under extreme weather.

(4) The extreme wind often accompanied by rain erosion and sudden changes in wind speed, further analysis should be incorporated into the future model parameters.

ACKNOWLEDGEMENT

This work was supported by Science and Technology Project of State Grid (5400-202216167A-1-1-ZN), Water conservancy science and technology plan project of Shaanxi Province (2021slkj-8).

REFERENCE

[1] "High-resolution data shows China's wind and solar energy resources are enough to support a 2050 decarbonized electricity system," Applied Energy, vol. 306, p. 117996, 2022/01/15/ 2022.

[2] M. Li, D. Patiño-Echeverri, and J. Zhang, "Policies to promote energy efficiency and air emissions reductions in China's electric power generation sector during the 11th and 12th five-year plan periods: Achievements, remaining challenges, and opportunities," Energy Policy, vol. 125, pp. 429-444, 2019/02/01/ 2019.

[3] M. Shademan, R. Balachandar, and R. M. Barron, "Detached eddy simulation of flow past an isolated inclined solar panel," Journal of Fluids and Structures, vol. 50, pp. 217-230, 2014/10/01/ 2014.

[4] W. Bender, D. Waytuck, S. Wang, and D. A. Reed, "In situ measurement of wind pressure loadings on pedestal style rooftop photovoltaic panels," Engineering Structures, vol. 163, pp. 281-293, 2018/05/15/ 2018.

[5] M. Asghari Mooneghi, P. Irwin, and A. Gan Chowdhury, "Partial turbulence simulation method for predicting peak wind loads on small structures and building appurtenances," Journal of Wind Engineering and Industrial Aerodynamics, vol. 157, pp. 47-62, 2016/10/01/ 2016.

[6] Z. Liu, Q. Tan, Y. Zhou, and H. Xu, "Syncretic Application of IBASBP Algorithm for Monitoring Equipment Online in Power System," IEEE Access, vol. 9, pp. 21769-21776, 2021.

[7] D. I. Ladas, T. Stathopoulos, and E. D. Rounis, "Wind effects on the performance of solar collectors on rectangular flat roofs: A wind tunnel study," Journal of Wind Engineering and Industrial Aerodynamics, vol. 161, pp. 27-41, 2017/02/01/ 2017.

[8] R. N. Pratt and G. A. Kopp, "Velocity measurements around low-profile, tilted, solar arrays mounted on large flat-roofs, for wall normal wind directions," Journal of Wind Engineering and Industrial Aerodynamics, vol. 123, pp. 226-238, 2013/12/01/ 2013.

[9] C. Geurts and P. Blackmore, "Wind loads on stand-off photovoltaic systems on pitched roofs," Journal of Wind Engineering and Industrial Aerodynamics, vol. 123, pp. 239-249, 2013/12/01/ 2013.

[10] D. Banks, "The role of corner vortices in dictating peak wind loads on tilted flat solar panels mounted on large, flat roofs," Journal of Wind Engineering and Industrial Aerodynamics, vol. 123, pp. 192-201, 2013/12/01/ 2013.